

Short communication

# Novel application of aluminum salt for cost-effective fabrication of a highly creep-resistant nickel–aluminum anode for a molten carbonate fuel cell

Hoonhee Lee<sup>a,\*</sup>, Insung Lee<sup>a</sup>, Dokyol Lee<sup>a</sup>, Heechun Lim<sup>b</sup>

<sup>a</sup> Division of Materials Science and Engineering, Korea University, 5-1 Anam-Dong, Sungbuk-Gu, Seoul 136-701, South Korea

<sup>b</sup> Korea Electric Power Research Institute, Daejeon 305-380, South Korea

Received 15 April 2006; accepted 30 July 2006

Available online 25 September 2006

## Abstract

A one-step sintering process using aluminum acetate as an aluminum source is used to fabricate a nickel-based anode for a molten carbonate fuel cell (MCFC). The process is designed to replace existing partial or full oxidation and reduction processes, which are quite complicated and expensive. The aim is to simplify the fabrication process of a highly creep-resistant Ni–Al anode and eventually to contribute to the commercialization of a MCFC. Considering the solubility limit of Al in Ni, two types of anodes, Ni–2.5 wt.%Al and Ni–5 wt.%Al, are fabricated by sintering at either 1000 or 1100 °C for 2 h in a 99.5% H<sub>2</sub> atmosphere. After characterizing the resulting material by X-ray diffraction, scanning electron microscopy and energy dispersive X-ray spectroscopy, it is confirmed that among the anodes fabricated, the Ni–5 wt.%Al sample sintered at 1100 °C contained the most suitable Al<sub>2</sub>O<sub>3</sub> in a dispersed form. A 100-h creep test reveals that the creep strain of the anode has the lowest value of 1.3% compared with the other anodes. This value is superior to the creep strain of 2.3% obtained from a Ni–5 wt.%Al anode using Al powder as a fine Al<sub>2</sub>O<sub>3</sub> dispersion source in a Ni-base anode matrix. A single cell using the Ni–5 wt.%Al anode fabricated in this study shows a stable closed-circuit voltage of 0.795 V for 1000 h at 150 mA cm<sup>-2</sup>.

© 2006 Elsevier B.V. All rights reserved.

**Keywords:** Molten carbonate fuel cell; Anode; Aluminum salt; Oxide dispersion strengthening; Creep resistance

## 1. Introduction

Extensive studies have been carried out over the past several decades with the ultimate aim of commercializing the molten carbonate fuel cell (MCFC) [1,2]. The system components and stack performances of MCFCs have been improved significantly and commercial demonstrations are being run by Fuel Cell Energy Inc. (FCE), in the USA [3]. Despite this recent progress, however, stack durability and fabrication costs are still critical issues that hinder the commercialization of MCFCs.

Among the components, the anode requires substantial improvement to solve the creep problem. Generally, a MCFC is operated at 923 K, which is  $\geq 50\%$  of the melting temperature ( $T_m$ ) of Ni. In addition, the MCFC stack is placed under a torque load, which is required to minimize the contact resistance between components. It should be noted that the bottom cells

of a 500-cell MCFC stack would experience a load of approximately 0.5 kg cm<sup>-2</sup> from the weight of the stack alone [4]. Above 0.5 $T_m$ , a metal will deform plastically over a period of time even when the applied stress is lower than its yield strength [5]. This time-dependent deformation is known as creep, and this is one of the main problems that limit the lifetime of an MCFC. Anode creep causes not only an unstable gas supply as a result of the variation in the pore structure and the reduction of porosity, but it can also increase the contact resistance between the anode and the electrolyte matrix due to local deformation of the anode. This ultimately lowers the power of the stack [4]. The mechanisms of this creep deformation are mainly divided into four groups, namely, dislocation glide, dislocation creep, diffusion creep and grain boundary sliding [6]. Lattice imperfections, such as solute atoms, precipitates or oxide particles, can block the movement and thereby suppress creep. This effect is known as strengthening. Therefore, most attempts made to enhance the creep resistance of an anode have employed one of the many imperfection-strengthening methods or a combination of them [7]. Aluminum, chromium and copper have been considered as

\* Corresponding author. Tel.: +82 2 3290 3813; fax: +82 2 928 3584.  
E-mail address: [eguitar97@naver.com](mailto:eguitar97@naver.com) (H. Lee).

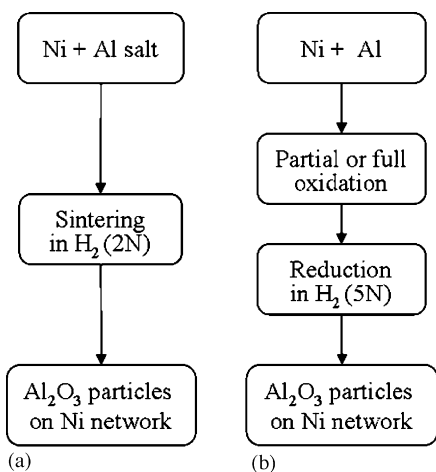


Fig. 1. Comparison of: (a) one-step and (b) partial or full oxidation–reduction sintering process.

a second element for strengthening a Ni-base anode and it has been reported that either a Ni–Al or Ni–Cr system has sufficient creep resistance [8,9], with the former being superior to the latter. According to our previous work [8], the creep resistance of Ni–Al anodes is improved considerably compared with a pure Ni anode prepared by solid solution or oxide dispersion via a partial or full oxidation and reduction sintering process (hereafter referred to as PR and FR). Indeed, using Al powder, PR or FR is an excellent method for producing an anode with a uniform  $\text{Al}_2\text{O}_3$  dispersion in the Ni-base anode matrix. On the other hand, it is very difficult to control precisely the atmosphere for partial oxidation, particularly in the large-scale sintering furnaces that are used for mass production. In addition, the PR or FR process is a two-step procedure, which complicates the sintering process and increases the expense. For commercialization, therefore, a novel anode with a high creep resistance needs to be fabricated by a simple process using low cost materials.

The aim of the work reported here is to develop an anode that has high creep resistance and is cost-effective. An Al salt (Al acetate) is used as the source for  $\text{Al}_2\text{O}_3$  formation to increase the creep resistance by dispersion strengthening. The main idea is that Al acetate dispersed homogeneously among Ni powders will be decomposed to  $\text{Al}_2\text{O}_3$  during the course of sintering and the resultant morphology will be a microstructure containing fine  $\text{Al}_2\text{O}_3$  dispersed in a Ni-base matrix. Hence, a complex process such as PR or FR is not required to make an oxide dispersion strengthened anode. Moreover, it is thought that the price of Al acetate could be lower than that of Ni–Al alloy from a mass production viewpoint. In this study, a one-step sintering procedure using ordinary hydrogen is used for economical fabrication of the anode. A comparison of the PR or FR with the one-step sintering procedure is given in Fig. 1.

## 2. Experimental

The decomposition phenomena of Al acetate were analyzed by thermal analysis using a thermogravimetric analyzer and a differential scanning calorimeter (TGA-DSC, TA instruments

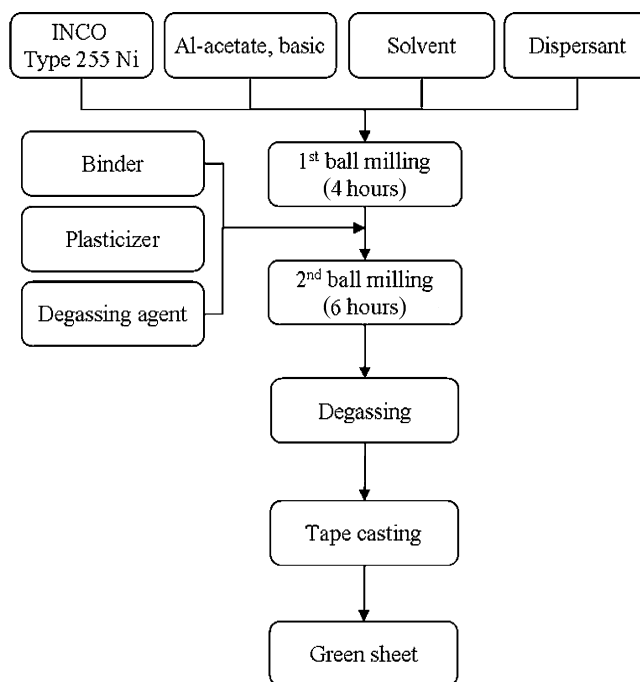


Fig. 2. Fabrication procedure for anode green sheets.

SDT 2960). The phases of the decomposed products were characterized by means of an X-ray diffractometer (XRD, Rigaku Geigerflex DMAX-IIA).

The anode composition was determined to be within the solubility limit of Al in Ni according to the findings of Kim et al. [8]. Ni–2.5 wt.%Al and Ni–5 wt.%Al anode green sheets were fabricated using filamentary Ni (Type 255, Inco) and Al acetate (Insoluble form, Sigma–Aldrich) as the starting materials, as shown in Fig. 2. An ethanol–water mixture, Disperbyk 110 (BYK-Chemie), dibutyl phthalate (SBC Co. Ltd.), B-72 polyvinyl butyral (Butvar) and SN-348 (Dappo) were used as the solvent, dispersant, plasticizer, binder and degassing agent, respectively.

The anode green sheets were then sintered at the selected temperature for 2 h in an ordinary hydrogen atmosphere (purity 99.5%). The sintered anodes were also characterized by XRD to identify the phases, and by a field emission scanning electron microscope (FE-SEM, Hitachi 6300) and an energy dispersive X-ray spectrometer (EDS, Oxford) to observe the morphology of the anode. The creep test was performed using the apparatus described elsewhere [8]; the tests conditions were 650 °C for 100 h in a  $\text{H}_2$  atmosphere under a load of 100 psi. The porosity was measured by means of the Archimedes method (ASTM, C373-72), and the pore-size distribution was obtained using a mercury porosimeter (Micromeritics, Autopore IV 9500). Single-cell tests were performed at 650 °C for 1000 h using a test station designed and constructed in Korea Institute of Science and Technology, South Korea (KIST) [10]. Gas mixtures containing 72%  $\text{H}_2$ –18%  $\text{CO}_2$ –10%  $\text{H}_2\text{O}$  and 70% air–30%  $\text{CO}_2$  were supplied to the anode and the cathode, respectively. The total flow rate of the gas was equivalent to a gas utilization of 40% at 150  $\text{mA cm}^{-2}$ .

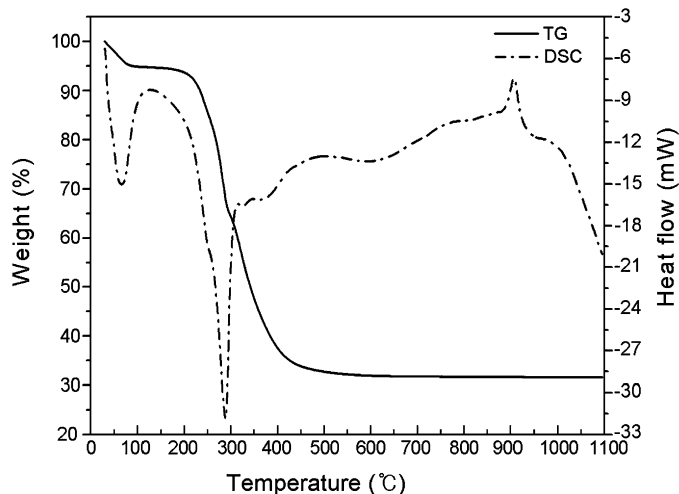


Fig. 3. TG-DSC curves of Al acetate.

### 3. Results and discussion

#### 3.1. Characterization of Al acetate

The average particle size of the Al acetate ( $\text{Al}(\text{OH})(\text{CH}_3\text{COO})_2$ ) powder was  $1\ \mu\text{m}$  [11] and it did not melt in the solvent used for tape-casting. Therefore, the Al acetate was distributed among the Ni powders in the form of a powder when the anode green sheets are fabricated. Hence, a uniform distribution of  $\text{Al}_2\text{O}_3$  in the Ni-base matrix is expected if there is a homogeneous dispersion of Al acetate powder with the subsequent formation of  $\text{Al}_2\text{O}_3$  during sintering. The formation of  $\text{Al}_2\text{O}_3$  was confirmed by thermal analysis and heat treatment. The Al acetate was heat-treated from 200 to  $1100\ ^\circ\text{C}$  at  $100\ ^\circ\text{C}$  intervals.

Figs. 3 and 4 show, respectively, thermogravimetric gravimetric and differential scanning gravimetric (TG-DSC) curves for Al acetate and XRD patterns of the Al acetate after heat treatment at various temperatures for 2 h in a  $\text{H}_2$  atmosphere. In

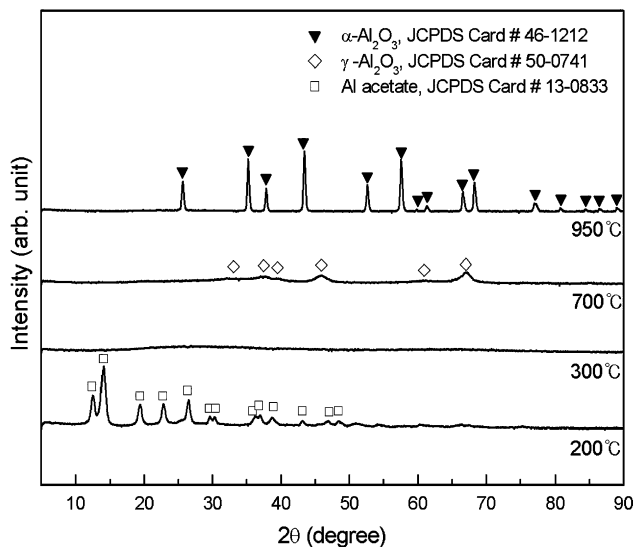


Fig. 4. XRD patterns of Al acetate after heat treatment at various temperatures for 2 h in  $\text{H}_2$  atmosphere.

Table 1

Change in porosities of Ni–2.5 wt.%Al and Ni–5 wt.%Al anode with sintering temperature

Specimen	Porosity (%)	
	At $1000\ ^\circ\text{C}$	At $1100\ ^\circ\text{C}$
Ni–2.5 wt.%Al	70	56
Ni–5 wt.%Al	73	60

Fig. 3, two endothermic peaks at approximately  $70$  and  $300\ ^\circ\text{C}$ , and two exothermic peaks at approximately  $900$  and  $1000\ ^\circ\text{C}$  are clearly visible. It is believed that the first endothermic peak and weight loss are caused by evaporation of water. Referring to the XRD pattern at  $200\ ^\circ\text{C}$  in Fig. 4, it is confirmed that the Al acetate phase is still present at  $200\ ^\circ\text{C}$ . The following endothermic peak and weight loss appear to be due to thermal decomposition of the organic components. Extensive weight loss occurs as the thermal decomposition is increased above  $200\ ^\circ\text{C}$ , and the phase becomes amorphous. Above  $700\ ^\circ\text{C}$ , the  $\gamma\text{-Al}_2\text{O}_3$  phase appears as a broad peak and this indicates incomplete thermal decomposition. Given the exothermic peaks at  $900$  and  $1000\ ^\circ\text{C}$ , it is expected that the final decomposition product will be formed at a temperature  $\geq 950\ ^\circ\text{C}$ . The  $\gamma$  to crystalline  $\alpha$  phase change in  $\text{Al}_2\text{O}_3$  is shown in Fig. 4. The results also suggest that  $\alpha\text{-Al}_2\text{O}_3$  can be formed from Al acetate in the anode green sheet by thermal decomposition at  $\geq 950\ ^\circ\text{C}$ .

#### 3.2. Phases and morphologies

Anode green sheets with two compositions, viz., Ni–2.5 wt.%Al and Ni–5 wt.%Al (hereafter referred to as NA2.5 and NA5, respectively), were fabricated and sintered by a one-step sintering procedure at either  $1000$  or  $1100\ ^\circ\text{C}$  for 2 h in a  $\text{H}_2$  atmosphere. Figs. 5 and 6 show the XRD patterns and SEM images of the NA2.5 and NA5 sintered at  $1000$  or  $1100\ ^\circ\text{C}$ . These data suggest that the  $\text{Al}_2\text{O}_3$  phase does not exist in the anodes sintered at  $1000\ ^\circ\text{C}$ , which is contrary to the results shown in Section 3.1. By contrast, for the anodes sintered at  $1100\ ^\circ\text{C}$ ,  $\text{Al}_2\text{O}_3$  peaks can be observed in the XRD patterns. Why is the  $\text{Al}_2\text{O}_3$  phase not seen in the XRD patterns of anodes sintered at a higher temperature than  $950\ ^\circ\text{C}$ , i.e., the formation temperature of  $\text{Al}_2\text{O}_3$  from Al acetate? It is judged that  $\text{Al}_2\text{O}_3$  can be formed at  $950\ ^\circ\text{C}$  when Al acetate is heat-treated alone, but when Al acetate is mixed with Ni in the anode green sheet, the quantity of crystalline components of  $\text{Al}_2\text{O}_3$  is below the detection limit of XRD. Therefore, the  $\text{Al}_2\text{O}_3$  phase may not be observed in XRD patterns of the anodes sintered at  $1000\ ^\circ\text{C}$ . On the other hand, the NA5 sintered at  $1100\ ^\circ\text{C}$  contains fine oxide particles dispersed in the anode, which is a morphology similar to that of the anode with a high creep resistance that has been reported [8] previously using Al powder.

The porosities of the above anodes were investigated to determine if they have the appropriate porosity for a MCFC anode; the results are shown in Table 1. NA2.5 and NA5 sintered at  $1000\ ^\circ\text{C}$  have a porosity of approximately 70%. It is considered that this porosity would be too high to resist the applied pressure

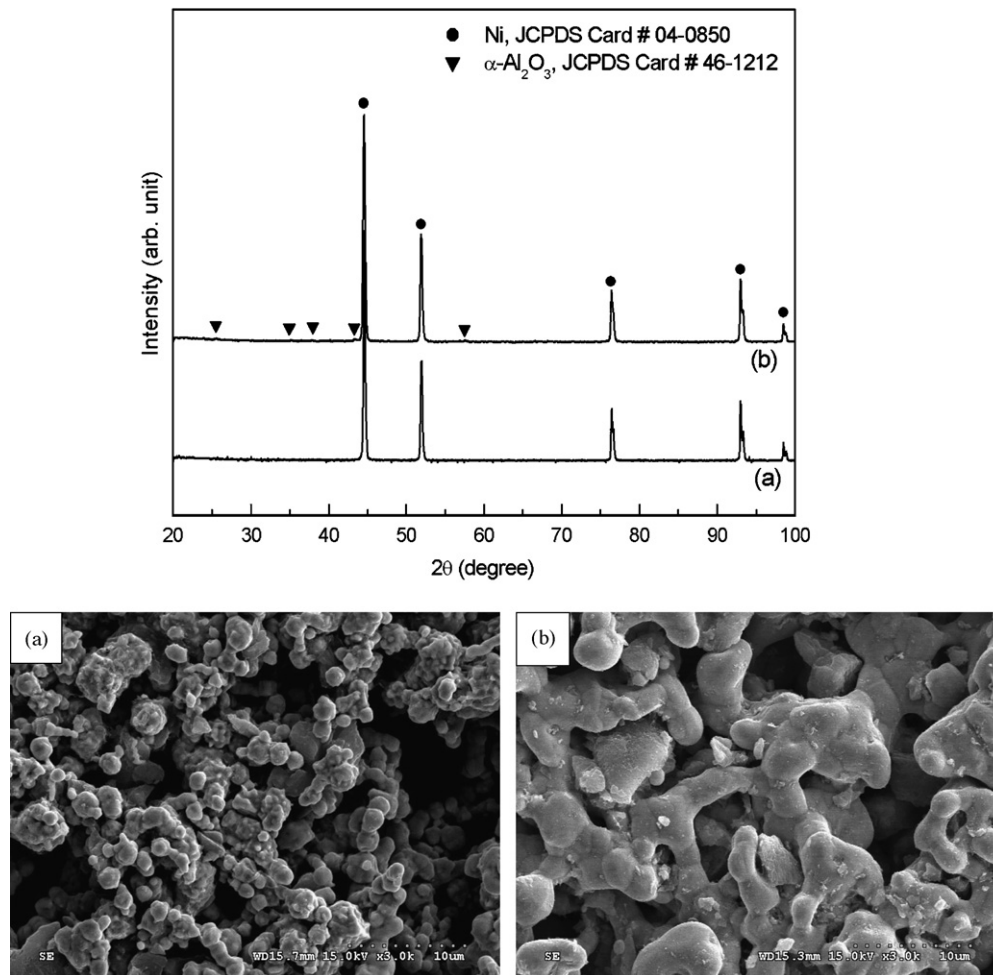


Fig. 5. XRD patterns and SEM images of Ni–2.5 wt.%Al anode sintered at: (a) 1100 °C and (b) 1000 °C for 2 h in H<sub>2</sub> atmosphere.

during the creep test [8]. Furthermore, the degree of sintering of the Ni particles is insufficient to shape the network structure, as shown in Figs. 5 and 6. For this reason, the anodes sintered at 1000 °C are excluded from subsequent analysis.

The porosity of the two anodes sintered at 1100 °C is within the range acceptable for a MCFC anode, but the average pore size of NA2.5 sintered at 1100 °C is smaller than that recommended for an anode. Another essential parameter for a MCFC anode is the pore-size distribution. The average pore size is usually 3–6 μm. The average pore size of the NA2.5 (porosity 56%) and NA5 (porosity 60%) was 2.6 and 3 μm, respectively. The pore-size distribution of the two anodes is shown in Fig. 7.

### 3.3. Creep behaviour and single-cell performance

The creep behaviour of the NA2.5 and NA5 sintered at 1100 °C was investigated using a creep test apparatus. The creep curves are given in Fig. 8. The creep strain of the two anodes after the creep test is estimated to be 4.1% for NA2.5 (porosity 56%) and 1.3% for NA5 (porosity 60%), respectively. Although the porosity of NA5 is higher than that of NA2.5, the former has a lower creep strain than the latter. Consequently, it is concluded that the Al<sub>2</sub>O<sub>3</sub> formed in the NA2.5 is insufficient to enhance the anode strength.

In a study of anodes with added Al powder [8], it was concluded that the strengthening mechanism was a combination of a solid solution and oxide dispersion strengthening that resulted in a very low anode creep strain of 2.3%. Given the expected life-time (40,000 h) of a MCFC stack, Al contained in the anode will be gradually oxidized by the impurities such as O<sub>2</sub> or H<sub>2</sub>O in the fuel gas. Therefore, it is believed that oxide dispersion strengthening is the final strengthening mechanism and that NA5 exhibits excellent creep resistance accordingly. A comparison of previous work using Al powder [8] with this study shows that the anode enhanced by oxide dispersion strengthening has a higher creep resistance as a result of a combination of two strengthening mechanisms. The results of the creep test for NA5 support the final strengthening mechanism proposed above.

Finally, a single-cell test was performed using NA5 at 150 mA cm<sup>-2</sup> for 1000 h. The initial single-cell performance showed an open-circuit voltage (OCV) of 1.065 and 0.799 V at 150 mA cm<sup>-2</sup>. The single-cell performance, namely, average 0.795 V at 150 mA cm<sup>-2</sup>, is stable during an operating time of 1000 h. Figs. 9 and 10 show the single-cell performance and closed-circuit voltage (CCV) at 150 mA cm<sup>-2</sup> as a function of time, respectively. The anode gives acceptable single-cell performance for a MCFC anode.

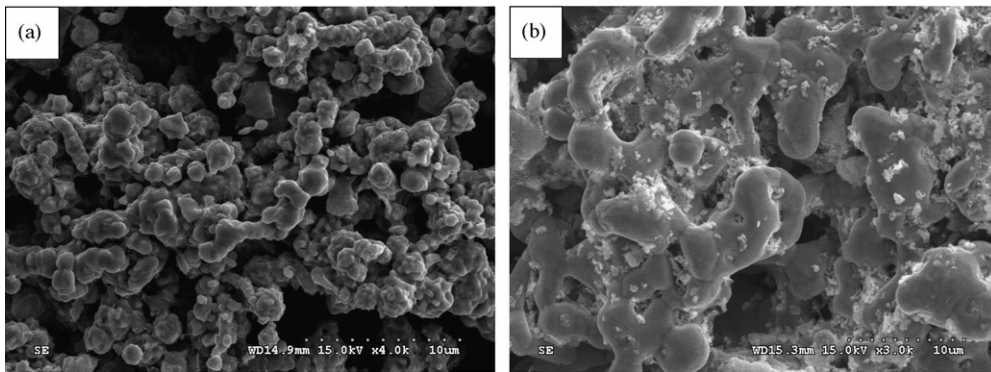
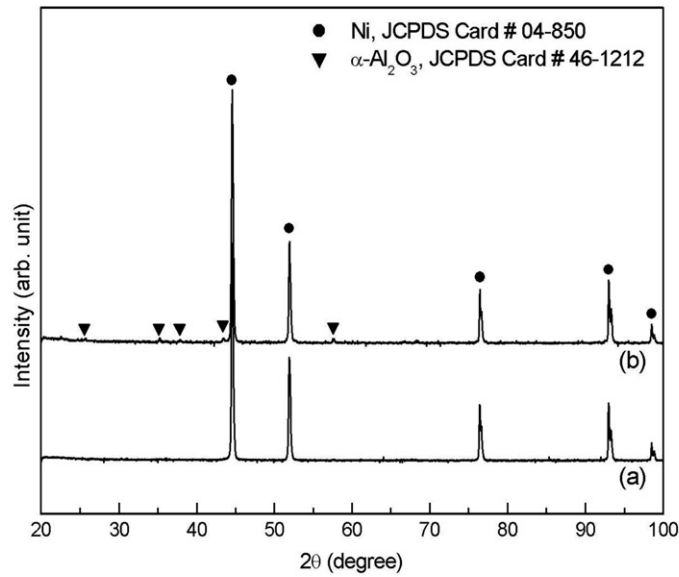


Fig. 6. XRD patterns and SEM images of Ni–5 wt.%Al anode sintered at: (a) 1100 °C and (b) 1000 °C for 2 h in H<sub>2</sub> atmosphere.

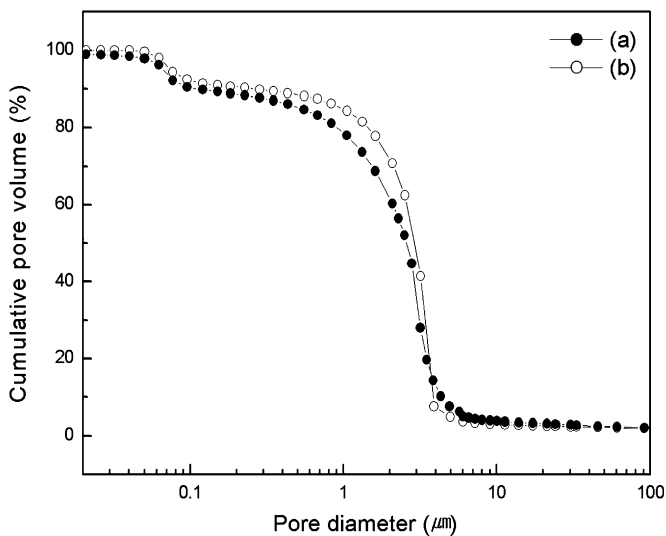


Fig. 7. Pore-size distribution of: (a) Ni–2.5 wt.%Al and (b) Ni–5 wt.%Al anode sintered at 1100 °C for 2 h in H<sub>2</sub> atmosphere.

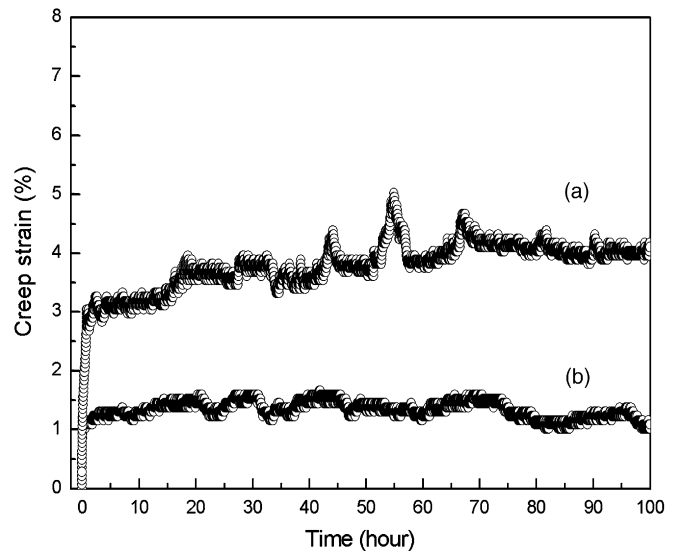


Fig. 8. Creep curves of: (a) Ni–2.5 wt.%Al and (b) Ni–5 wt.%Al anode sintered at 1100 °C for 2 h in H<sub>2</sub> atmosphere.

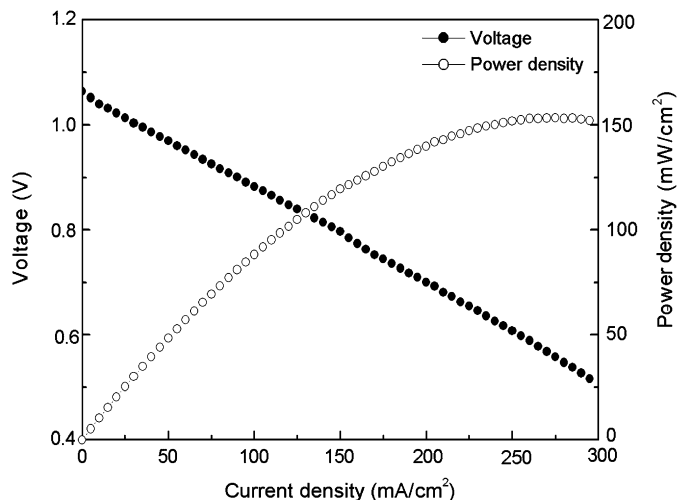


Fig. 9. Single-cell performance of a Ni-5 wt.%Al anode sintered at 1100 °C for 2 h in H<sub>2</sub> atmosphere.

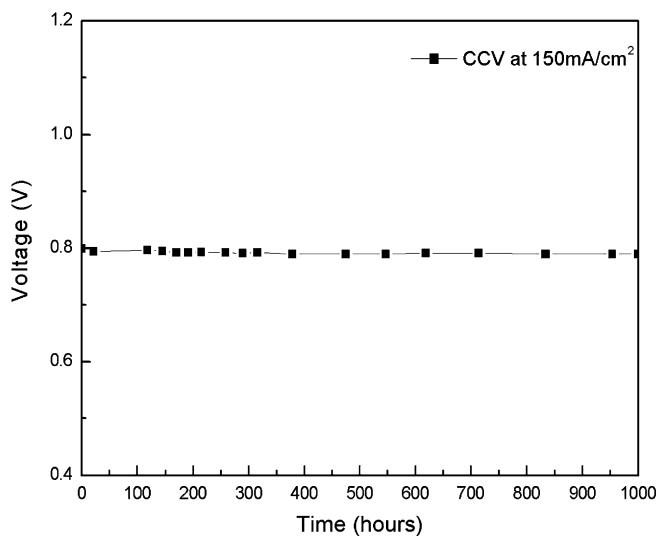


Fig. 10. Single-cell performance as function of time using Ni-5 wt.%Al anode sintered at 1100 °C for 2 h in H<sub>2</sub> atmosphere.

#### 4. Conclusions

$\alpha$ -Al<sub>2</sub>O<sub>3</sub> dispersed in a Ni-2.5 wt.%Al and Ni-5 wt.%Al anode has been achieved by adding Al acetate via a one-step

sintering procedure in an ordinary H<sub>2</sub> (99.5%) atmosphere. The morphologies, creep behaviour, and single-cell performance are investigated. The Al acetate forms an  $\alpha$ -Al<sub>2</sub>O<sub>3</sub> phase as a result of thermal decomposition at temperatures  $\geq 950$  °C. A Ni-base anode with fine Al<sub>2</sub>O<sub>3</sub> particles dispersed uniformly has been fabricated using a cost-effective one-step sintering process. A Ni-5 wt.%Al anode sintered at 1100 °C using Al acetate exhibits a higher creep resistance (creep strain of 1.3%) than that of an anode examined elsewhere (creep strain of 2.3%). A single cell with a Ni-5 wt.%Al anode sintered at 1100 °C gives an average voltage of 0.795 V over 1000 h. The application of an Al salt and a one-step sintering procedure using a H<sub>2</sub> (99.5%) atmosphere is expected to be a less expensive procedure than those currently used.

#### Acknowledgements

This study was financially supported by The Korea Electric Power Corporation and The Korea Ministry of Commerce, Industry and Energy, through the development of 250-kW MCFC system. The authors are grateful to staff in the Fuel Cell Research Center at KIST for assistance in performing single-cell tests.

#### References

- [1] J. Larminie, A. Dicks, *Fuel Cell Systems Explained*, John Wiley & Sons Ltd., England, 2000, pp. 161–164.
- [2] W. Vielstich, A. Lamm, H.A. Gasteiger (Eds.), *Handbook of Fuel Cells-Fundamentals, Technology and Applications*, vol. 1, John Wiley & Sons Ltd., England, 2003, pp. 221–224.
- [3] G. Steinfeld, J. Hunt, Fuel Cell Energy Inc.; P.M. Sööt, Northwest Fuel Development Inc.
- [4] A.J. Appleby, F.R. Foulkes, *Fuel Cell Handbook*, Van Nostrand Reinhold, New York, 1988, pp. 568–570.
- [5] C.R. Barret, A.S. Tetelman, W.D. Nix, *The Principles of Engineering Materials*, Prentice-Hall, Englewood Cliff, NJ, 1973, pp. 215.
- [6] G.E. Dieter, *Mechanical Metallurgy*, third ed., McGraw-Hill, New York, 1986 (Chapter 13).
- [7] Dohwon Jung, Insung Lee, Heechun Lim, Dokyol Lee, *J. Mater. Chem.* 13 (2003) 1717–1722.
- [8] Gyubeom Kim, Youngjoon Moon, Dokyol Lee, *J. Power Sources* 104 (2002) 181–189.
- [9] Dokyol Lee, Dohwon Jung, Insung Lee, Kyungrae Byun, Heechun Lim, *Met. Mater. Int.* 9 (6) (2003) 605–611.
- [10] Seungwoo Kim, Sungpil Yoon, Jonhee Han, Sukwoo Nam, Taehoon Lim, Seongahn Hong, Heechun Lim, *J. Power Sources* 112 (2002) 109–115.
- [11] Insung Lee, Wonsun Kim, Youngjoon Moon, Heechun Lim, Dokyol Lee, *J. Power Sources* 101 (2001) 90–95.